Journal of Solid State Chemistry 183 (2010) 1805–1810

Contents lists available at ScienceDirect

Journal of Solid State Chemistry

journal homepage: www.elsevier.com/locate/jssc

Magnetic properties of linear trimers in fluoride analogs of tetragonal tungsten bronze

Yaw-Shun Hong [1], William O.J. Boo [2], Daniell L. Mattern *

Department of Chemistry and Biochemistry, University of Mississippi, University, MS 38677, USA

ARTICLE INFO

Article history:
Received 8 January 2010
Received in revised form
27 April 2010
Accepted 22 May 2010
Available online 2 June 2010

Keywords:
Linear trinuclear complexes
Linear trimers
Tetragonal tungsten bronze
Ionic ordering
Magnetic coupling
Magnetic susceptibility

ABSTRACT

The compounds $KZnTiF_6$, $KZnVF_6$, $KVScF_6$, $KCrScF_6$, and $KMnScF_6$ are fluoride analogs of Tetragonal Tungsten Bronze. M^{2+}–M^{3+} ionic ordering in these fluorides provided systems which contained linear trinuclear complexes of their respective paramagnetic ions. Magnetic coupling within these linear trimers occurred below 100 K in each of the five systems. Derived magnetic susceptibility equations were fitted to observed magnetic susceptibilities for each of the possible spin systems: $KZnTiF_6$ ($S=1/2$), $J/k=-114$ K; $KZnVF_6$ ($S=1$), $J/k=-39$ K; $KVScF_6$ ($S=3/2$), $J/k=-16$ K; $KCrScF_6$ ($S=2$), $J/k=-4$ K; and $KMnScF_6$ ($S=5/2$), $J/k=-7.5$ K.

1. Introduction

The structure of tetragonal tungsten bronze (TTB) reported by Magneli [1], K_xWO_3 ($x=0.40$–0.60), belongs to space group D^5_{4h}-$P4/mbm$. In the TTB structure (Fig. 1a), tungsten ions occupy all 8*j* and 2*c* sites. $K_{0.54}Mn_{0.54}Fe_{0.46}F_3$, a fluoride analog of TTB reported by Banks et al. [2], belongs to space group C^8_{4v}-$P4_2bc$. In this structure, variations in M–F distances show that Mn^{2+} ions occupy one set of 8*c* sites, and Fe^{3+} ions occupy a second set of 8*c* sites; this ordering of Mn^{2+} and Fe^{3+} ions doubles the *c* dimension of the unit cell. The 4*b* sites are randomly occupied by Mn^{2+} and Fe^{3+} ions within the *ab* plane, but are ordered along the *c* direction. This M^{2+}–M^{3+}–M^{2+}–M^{3+} ordering assures that M^{2+} ions have only M^{3+} ions for nearest neighbors along the *c* axis, and vice versa. Hong et al. [3] concluded that M^{2+}–M^{3+} ionic ordering (as illustrated in Fig. 1b) is common in first row transition metal fluorides having the TTB structure. The chemical formula for these compounds is $K_xM^{II}_xM^{III}_{1-x}F_3$, where $x=0.4$–0.6.

Such ionic ordering makes it possible to design materials with interesting magnetic properties [3]. First row transition metal fluorides have innate characteristics favorable for these studies. The fluoride ion is a weak ligand; hence, the transition metal ions have high-spin configurations. In the TTB structure, the transition metal ions are octahedrally coordinated, which are ideal for isotropic Landé factors (*g* values). Furthermore, a wide variety of M^{2+},M^{3+} combinations are possible in fluoride analogs of TTB. We have chosen five combinations, varying in spin, for study: Zn^{2+},Ti^{3+} ($S=1/2$); Zn^{2+},V^{3+} ($S=1$); V^{2+} ($S=3/2$), Sc^{3+}; Cr^{2+} ($S=2$), Sc^{3+}; and Mn^{2+} ($S=5/2$), Sc^{3+}. The Zn^{2+} and Sc^{3+} ions are diamagnetic.

Suppose that M^{2+} is paramagnetic and M^{3+} is diamagnetic. For composition $x=0.40$, all 8*c*(2) sites and all 4*b* sites would be occupied by M^{3+} ions. The M^{2+} ions, which are only on 8*c*(1) sites, would, to a first approximation, be magnetically isolated (Fig. 2a; only the M^{2+} and M^{3+} ions are shown). For composition $x=0.60$, along with the 8*c*(1) sites, all 4*b* sites would be occupied by M^{2+} ions; these ions would now all exist in linear trinuclear complexes (linear trimers) (Fig. 2c).

Fluoride analogs of TTB with $x=0.60$ would seem to be an ideal system for studying the magnetic behavior of such linear trimers. There are, however, two limitations with this composition. First, the linear trimers would all have nearest-neighboring M^{2+} ions along the *c* direction. Secondly, the fluoride analogs of TTB seldom form over the entire range of *x* (0.40–0.60) [3]. The composition closest to ideal is $K_{0.50}M^{II}_{0.5}M^{III}_{0.5}F_3$ ($=KM^{II}M^{III}F_6$) (Fig. 2b). Note that the unit cell contains ten M^{2+} ions and ten M^{3+} ions, since it comprises two of the layers shown in Fig. 2b. Eight of the M^{2+} ions are located on 8*c*(1) sites, and two are on 4*b* sites. Four of the M^{2+}

* Corresponding author. Fax: +1 662 915 7300.
E-mail addresses: yshong@ccit.edu.tw (Y.-S. Hong), mattern@olemiss.edu (D.L. Mattern).
[1] Present address: Department of Applied Chemistry, Chung Cheng Institute of Technology, Ta-Hsi, Taoyuan 33509, Taiwan. R.O.C.
[2] Author to whom questions should be addressed.

0022-4596/$ - see front matter © 2010 Elsevier Inc. All rights reserved.
doi:10.1016/j.jssc.2010.05.030

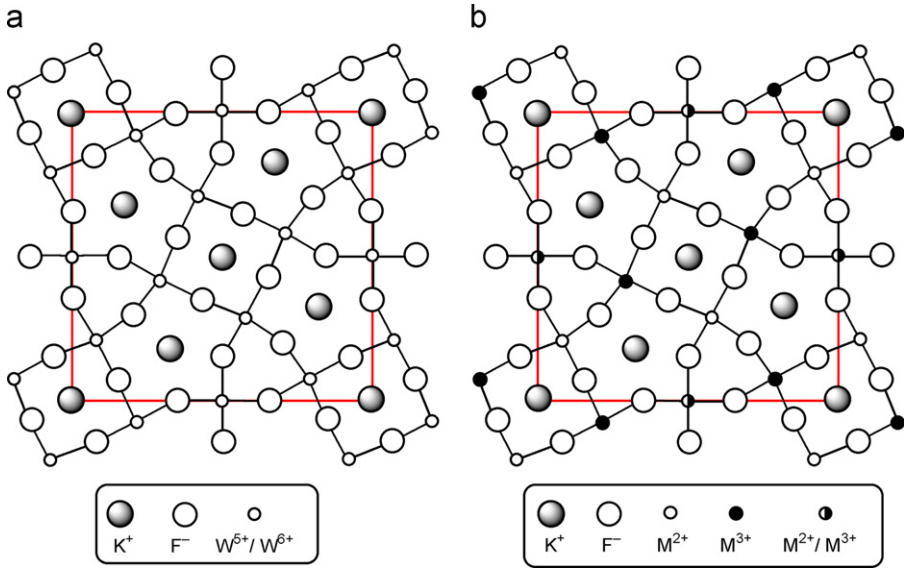

Fig. 1. (a) Structure of TTB, K_xWO_3 (x=0.4–0.6), showing positions of W^{5+}/W^{6+} ions on 8*j* and 2*c* sites. (b) Ionically ordered structure of $K_xM^{II}_xM^{III}_{1-x}F_3$, showing the positions of M^{2+} ions on 8*c*(1) sites, M^{3+} ions on 8*c*(2) sites, and mixed M^{2+}/M^{3+} ions on 4*b* sites.

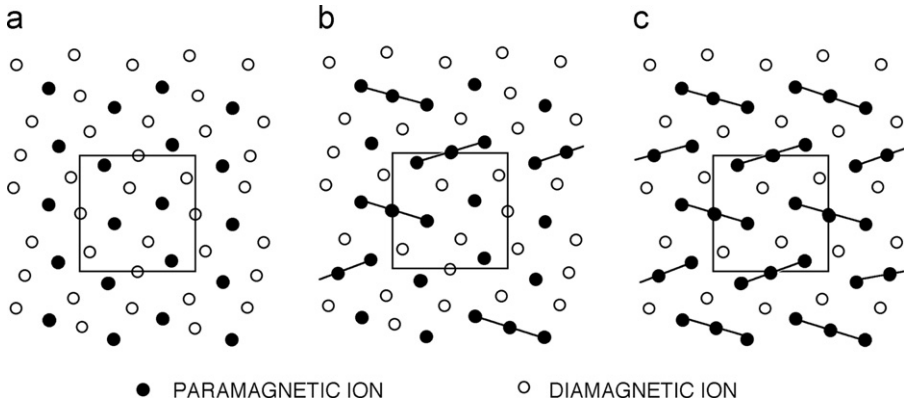

Fig. 2. Emergence of linear trimers in first-row transition metal fluoride analogs of TTB with composition $K_xM^{II}_xM^{III}_{1-x}F_3$ (x=0.4–0.6). Only M^{2+} and M^{3+} ions are shown. (a) When x=0.4, there are no linear trimers. (b) When x=0.5, six of every ten paramagnetic ions are associated with linear trimers; the other four paramagnetic ions are isolated, and (c) When x=0.6, all of the paramagnetic ions are in linear trimers.

ions on 8*c*(1) sites belong to linear trimers and four do not, that is, half of the paramagnetic ions located on 8*c*(1) sites are isolated. Both of the M^{2+} ions on 4*b* sites are central ions of linear trimers. To summarize, six of every ten M^{2+} ions belong to linear trimers while four, having no nearest-neighboring M^{2+} ion, do not. No magnetic coupling should occur with the four isolated M^{2+} ions, allowing them to remain paramagnetic over the entire temperature range (4.2–300 K). However, the M^{2+} ions within the linear trimers couple antiferromagnetically at low temperature, so that those three ions together display the same resultant spin as a single isolated M^{2+} ion.

An idealized plot of the inverse of the magnetic susceptibility χ_M^{-1} vs. temperature T for $KM^{II}M^{III}F_6$ (Fig. 3) reveals three distinct temperature regions. At high temperatures (Region I) there are ten paramagnetic M^{2+} ions per unit cell, each with spin=S. This region obeys the Curie–Weiss Law

$$\chi_M(\text{observed}) = C_M/(T\text{-}\theta) \quad (1)$$

where C_M is the Curie constant and θ the Weiss constant. At intermediate temperatures (Region II), magnetic coupling develops within the linear trimers. At low temperatures (Region III), magnetic coupling is complete, and six of the M^{2+} ions in the unit cell have been transformed into two linear trimers, each with a resultant spin=S. The two linear trimers and the four isolated paramagnetic ions make a total of six magnetic species per unit cell. Region III also obeys the Curie–Weiss Law

$$\chi_M(\text{observed}) = C'_M/(T-\theta') \quad (2)$$

but with new values of the Curie constant C'_M and the Weiss constant θ'.

Because there are ten magnetic species in Region I but only six in Region III, the ratio C'_M/C_M should equal 0.60 [3,4]. Ideally, θ' would be zero, implying that magnetic interactions between the ordered trimers and the uncoupled M^{2+} ions are insignificant. The Region III molar magnetic susceptibility χ_M(observed) of each compound should reflect the contributions of 0.60 mol of paramagnetic ions within linear trimers and 0.40 mol of isolated paramagnetic ions. A value for χ_M(calculated) may therefore be devised by adding together approximations of the two parts (Eq. (3)). Note that χ_{3M}(trimer) represents a contribution from 3 mol

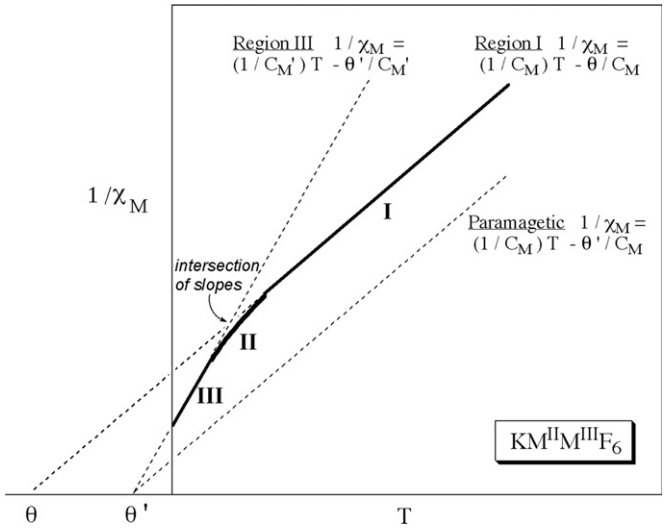

Fig. 3. Format of inverse magnetic susceptibility vs. temperature plots for $KM^{II}M^{III}F_6$. There are two linear regions, each of which has magnetic parameters. Curie–Weiss constants C_M and θ correspond to high temperatures (Region I); C'_M and θ' correspond to low temperatures (Region III). Magnetic coupling within linear trimers sets in at intermediate temperatures (Region II). The $1/\chi_M$ paramagnetic line, which is hypothetical, represents 1 mol of uncoupled paramagnetic ions.

of paramagnetic ions but that coupling cancels 2/3 of their spin contribution. Note also that χ_M(paramagnetic) refers only to those paramagnetic ions that are isolated.

$$\chi_M(\text{calculated}) = 0.60[1/3\chi_{3M}(\text{trimer})] + 0.40\chi_M(\text{paramagnetic}) \quad (3)$$

Although there have been only a few examples of linear trinuclear complexes reported in the literature [5,6], the theoretical treatment of these complexes is extensive. A recipe for deriving χ_{3M}(trimer) equations for spin-only linear trinuclear complexes has been presented by Mabbs and Machin [7]. Since the central ion of a linear trimer is not equivalent to the terminal ions, they employ Kambe's method [8]. We have followed their recipe to derive equations for $S=1/2$, 1, 3/2, 2, and 5/2. The equations (Table S1, Supplementary Materials) had to be altered to account for the non-zero θ' values. This was done by replacing T in each equation by the imaginary temperature $T-\theta'$. A similar θ' correction was also necessary for χ_M(paramagnetic); that is,

$$\chi_M(\text{paramagnetic}) = C_M/(T-\theta') \quad (4)$$

Using the equations in Table S1 to calculate χ_{3M}(trimer) for each compound requires values for C_M, θ', g, and J/k. Values for C_M and θ' are obtained from plots like Fig. 3. Values for g are obtained from Eq. (5) [9].

$$g = \left[3kC_M/(N\beta^2 S[S+1])\right]^{1/2} \quad (5)$$

Values for J/k are obtained by successively improving the estimates of J/k at one temperature (e.g., 100 K) until a best fit is obtained of χ_M(calculated) with χ_M(observed). The resulting best-fit value of J/k is then used in the appropriate Table S1 equation over the entire temperature range of 4.2–300 K. This allows the construction of plots of χ_M^{-1}(calculated) vs. T for each compound, using Eq. (3).

2. Materials and methods

The preparations of VF_2 [10], VF_3 [10], and CrF_2 [11] have been described earlier. MnF_2 and ZnF_2 were prepared from carbonates covered with water in a Teflon beaker. Aqueous HF, 50% by weight, was added until the pH reached 6. The fluoride precipitates were dried in Teflon dishes at 110 °C. The remaining water was removed by placing the samples in graphite boats in a graphite-lined nickel furnace tube and passing HF over them for 2 h at 250 °C. Reagent grade ScF_3 and TiF_3 and optical grade KF were obtained commercially.

Stoichiometric amounts of KF, $M^{II}F_2$, and $M^{III}F_3$ were tared, pulverized, and thoroughly mixed. Samples were vacuum encapsulated in Mo containers by electron beam welding techniques. The sealed samples were fired at 800 °C for 24 h. Weight checks were made after each step to ensure that compositions of products were unchanged from nominal values. All samples were examined by optical microscopy for homogeneity and impurities to ensure there was no reaction between the products and the container material. X-ray powder diffraction data were obtained by Guinier–Hagg techniques using Cu$K\alpha_1$ radiation with Si as an internal standard. Precision lattice constants were determined by least-squares analyses. The data are presented in the Supplementary Materials as Table S2.

Magnetic susceptibilities were measured from 4.2 to 300 K using a PAR Foner type vibrating sample magnetometer equipped with a liquid helium cryostat and gallium arsenide temperature controller. Magnetic fields were measured with a model 8860 F.W. Bell Hall probe gaussmeter. Powder samples of approximately 50 mg were measured at a constant field of 10,000 G.

3. Results

All samples appeared single phased and homogeneous. X-ray analyses confirmed the formation of the TTB structure in each case. Lattice parameters of the five crystal structures are given in Table 1. In first row transition metal fluorides having the TTB structure, the ratio a/c is usually approximately 1.60 [3]. The a/c ratios for $KZnTiF_6$ and $KCrScF_6$ deviated somewhat from 1.60, providing examples of Jahn–Teller distortions that do not lower the space group symmetry.

Plots of χ_M^{-1} vs. T (both observed and calculated) for $KZnTiF_6$, $KZnVF_6$, $KVScF_6$, $KCrScF_6$, and $KMnScF_6$ are shown in Figs. 4–8, respectively. The calculated curves are generally in very good agreement with the experimental data; for $KZnTiF_6$ (Fig. 4) the data points scatter somewhat above 150 K due to the decrease in magnitude of the magnetic moment of Ti^{3+}. Magnetic coupling of all five compounds occurred between 4.2 and 100 K, as indicated by the non-linear regions of χ_M^{-1} vs. T seen in these figures.

Determinations of the magnetic parameters C_M, θ, C'_M, and θ' were made from these plots; the values are given in Table 1. All θ and θ' values are negative (except for the θ' of $KVScF_6$, which is zero), indicating that the exchange integrals were antiferromagnetic [9]. For $KZnTiF_6$, $KCrScF_6$, and $KMnScF_6$ the θ' of -5 K indicates that there were additional magnetic interactions between trimers and the uncoupled paramagnetic ions; for $KZnVF_6$, the θ' value of -9 K suggests that the magnetic interactions between the trimers and uncoupled V^{3+} ions were relatively large. The C'_M/C_M ratios (Table 1) were all close to 0.60, supporting the conclusion that linear trimers were formed [3]. The intersection of slopes (the point where Region I and Region III lines cross in Fig. 3) represents the regional temperature where linear trimers are formed; these temperatures (Table 1) ranged

Table 1
Lattice and magnetic parameters.

Compound	Lattice constants (±0.05%) (Å)	a/c	C_M (cm³ K/mol)	C'_M (cm³ K/mol)	θ (K)	θ' (K)	C'_M/C_M	g	Intersection of slopes (K)	J/k (K)
$KZnTiF_6$	12.593 7.962	1.58	0.292	0.173	−80	−5	0.592	1.76	80	−114
$KZnVF_6$	12.548 7.850	1.60	0.955	0.574	−65	−9	0.601	1.95	65	−39
$KVScF_6$	12.882 8.035	1.60	1.86	1.12	−34	0	0.602	1.99	50	−16
$KCrScF_6$	13.053 7.954	1.64	3.25	1.97	−18	−5	0.606	2.08	23	−4
$KMnScF_6$	12.996 8.111	1.60	4.37	2.64	−44	−5	0.604	2.00	50	−7.5

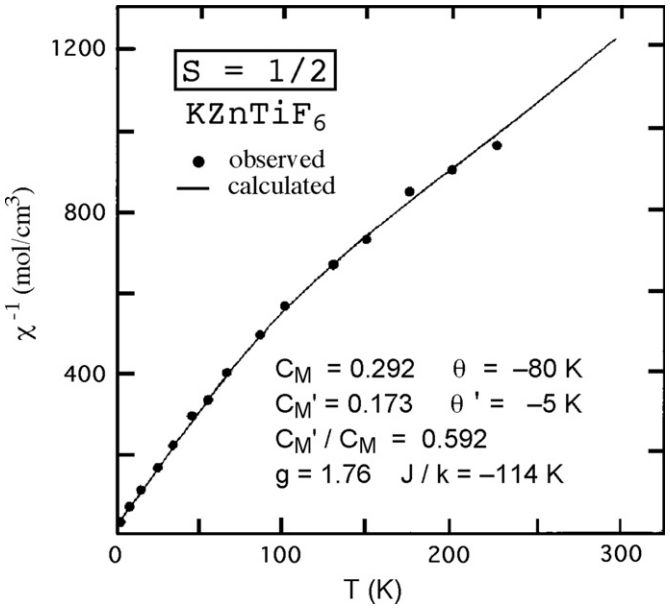

Fig. 4. Observed and calculated values of χ_M^{-1} vs. T for $KZnTiF_6$.

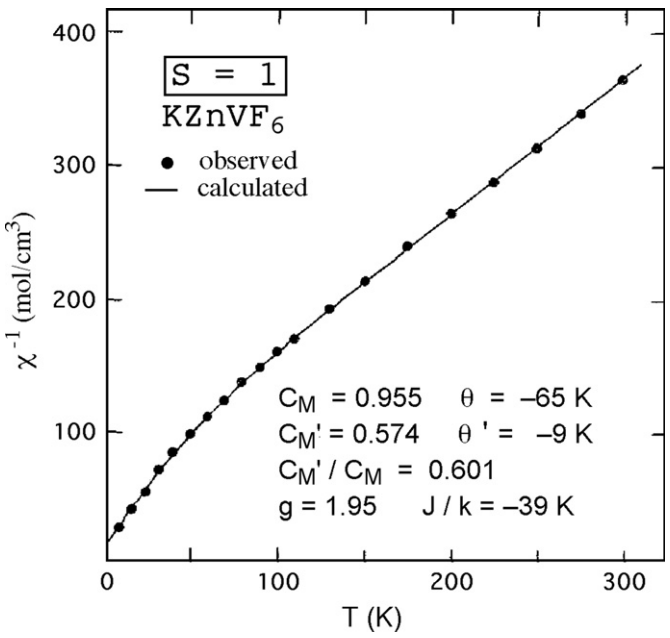

Fig. 5. Observed and calculated values of χ_M^{-1} vs. T for $KZnVF_6$.

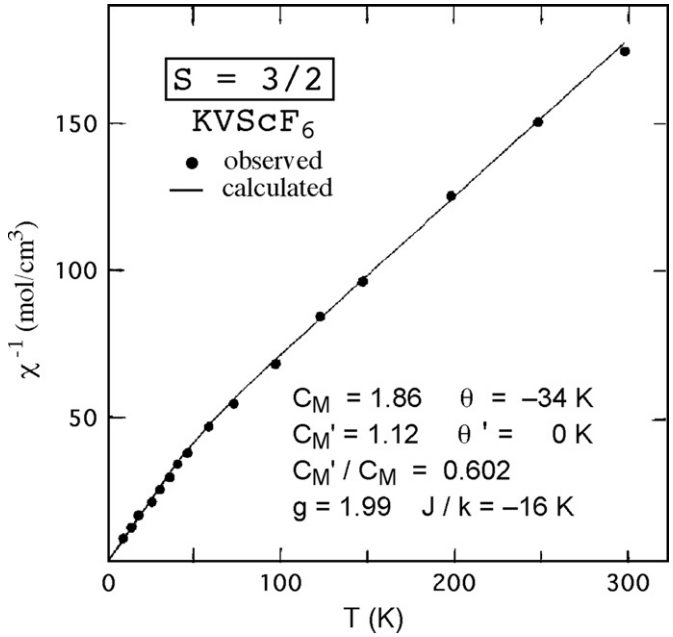

Fig. 6. Observed and calculated values of χ_M^{-1} vs. T for $KVScF_6$.

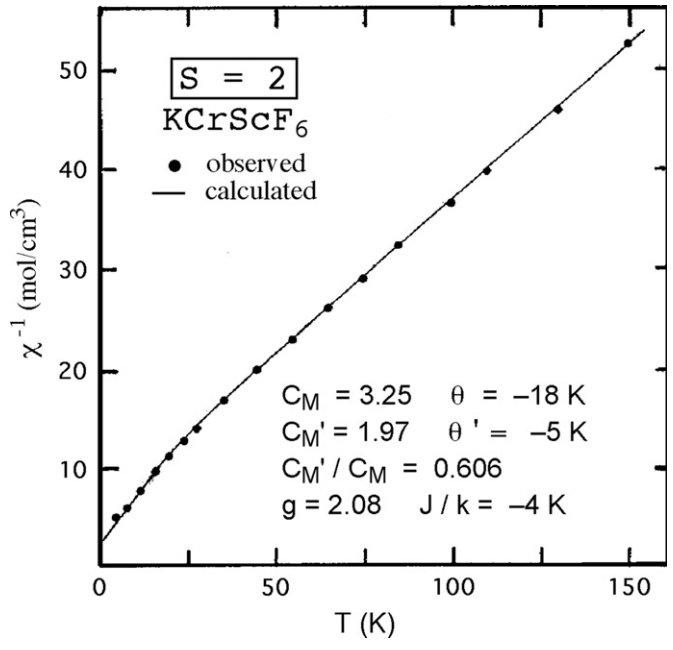

Fig. 7. Observed and calculated values of χ_M^{-1} vs. T for $KCrScF_6$.

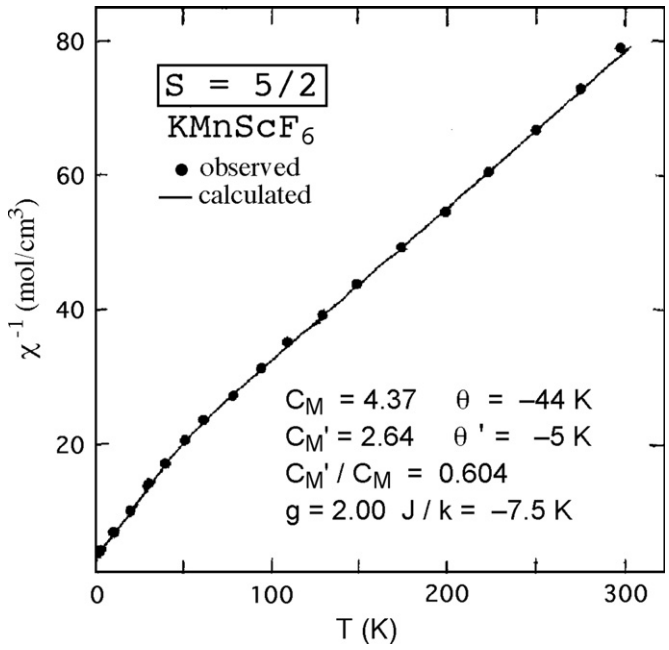

Fig. 8. Observed and calculated values of χ_M^{-1} vs. T for $KMnScF_6$.

from 23 to 80 K. Eq. (5) was used to obtain g values (Table 1); only the g value for $KZnTiF_6$ (1.76) is very far from the free electron value of 2.00.

For each of the five compounds, χ_M(calculated) values were determined using Eq. (3), with χ_{3M}(trimer) values estimated using the equations in Table S1 and χ_M(paramagnetic) values derived from the experimental parameters in Eq. (4). The J/k values used in the Table S1 equations were varied in each case at 100 K until χ_M(calculated) gave a best fit with χ_M(observed); the best-fit J/k values are given in Table 1. These values range from -114 to -4 K; the negative values indicated an antiferromagnetic exchange within the trimers [7].

4. Discussion

Each of the five compounds studied formed fluoride analogs of TTB. The Jahn–Teller ions Ti^{3+} and Cr^{2+} each distorted the TTB lattice as seen by the a/c ratios; Ti^{3+} decreased the ratio and Cr^{2+} increased it. Neither of the distortions, however, lowered the space group symmetry. The ratio $C_M'/C_M \sim 0.60$ supports the conclusions that ionic ordering is the same as that reported for $K_{0.54}Mn_{0.54}Fe_{0.46}F_3$ [2], and that linear trimers were formed [3,4]. After making corrections for uncoupled paramagnetic ions and non-zero θ', a fit of χ_M(calculated) with χ_M(observed) was obtained for each of the five compounds from the respective equations derived from the recipe by Mabbs and Machin [7].

The linear trinuclear complexes previously described in the literature, $[Ni(acetylacetonato)_2]_3$ [5] and $[Co_3(phcina)_6(quinoline)_2]$ [6], provide little basis for comparison with the linear trimers in the $KM^{II}M^{III}F_6$ compounds. Comparisons with the M–F–M magnetic interactions reported in other transition metal fluoride compounds can, however, provide valuable insight.

$S=1/2$: $KZnTiF_6$. Comparisons of the magnetic behavior of $KZnTiF_6$ with that of $BaTiF_5$ and $CaTiF_5$ reported by Eicher and Greedan [12] are interesting. The Ti^{3+} ions in each of the three compounds are octahedrally coordinated by F^- ions. In $BaTiF_5$ the octahedra exist in edge-sharing pairs, but in $CaTiF_5$ they form corner-sharing infinite linear chains. C_M values for $BaTiF_5$ and $CaTiF_5$ are 0.200 and 0.345, respectively, as opposed to 0.292 for $KZnTiF_6$. Since the octahedra of the linear trimers are corner sharing, one might expect some correlation between the magnetic behavior of $KZnTiF_6$ and $CaTiF_5$. However, magnetically coupled linear trimers of $KZnTiF_6$ form around 80 K, whereas no magnetic coupling was observed in either $CaTiF_5$ or $BaTiF_5$ above 4.2 K. The θ value of $KZnTiF_6$ is -80 K but it is approximately zero for the other two compounds. These differences in behavior probably mean that the single unpaired electron of Ti^{3+} is oriented differently in each of the three compounds.

$S=1$: $KZnVF_6$. The C_M values associated with V^{3+} in various fluoride structures differ significantly. Compounds having the general formula $A_xV_x^{II}V_{1-x}^{III}F_3$ (A=K, Rb, Cs, or Tl; x=0–1) include three structural types, all of which contain corner-sharing VF_6 octahedra: hexagonal tungsten bronze, TTB, and modified pyrochlore. For these three structural types, the values of $C_M(V^{3+})$ were approximated using the relationship

$$C_M(\text{observed}) = xC_M(V^{2+}) + (1-x)C_M(V^{3+})$$

In each case, $C_M(V^{2+})$ was taken to be 1.88. In the hexagonal bronze phases, $C_M(V^{3+})$ averaged 0.74 [13]. In the TTB phase, $C_M(V^{3+})$ values averaged 0.98 [14], and, within the limits of x, in the modified pyrochlore phases the average values of $C_M(V^{3+})$ were 0.74 for low x and 0.96 for high x [15]. Although $C_M(V^{3+})$ values differ slightly for different structures, there is strong agreement between the values of $KZnVF_6$ (0.955) and KV_2F_6 (0.98), both of which have the TTB structure. Clearly, the extent of orbital quenching of the V^{3+} ion is sensitive to small changes of its octahedral environment.

The temperatures at which magnetic couplings occur also reflect a similarity between $KZnVF_6$ and KV_2F_6. The average Néel temperature (T_N) for the hexagonal bronze phase was 8 K, for the TTB phase 50 K, and for the modified pyrochlore phase 10 K. Magnetic coupling in $KZnVF_6$ occurred around 65 K, which is clearly closest to the TTB-phase KV_2F_6.

$S=3/2$: $KVScF_6$. Several divalent fluorides of vanadium have been reported in the literature; g values of these compounds are consistently close to 2.00. Long range antiferromagnetic ordering, however, sets in over a wide range of temperatures: VF_2 (7 K) [10], $NaVF_3$ (35 K) [16,17], KVF_3 (130 K) [16,17], and $RbVF_3$ (120 K) [16]. The low T_N for VF_2 is a consequence of strong antiferromagnetic interactions between nearest neighbors (edge-sharing octahedra) along the c axis (V–F–V bond angles $\sim 90^\circ$, $J/k=-9$ K) with much weaker antiferromagnetic interactions between second nearest neighbors (V–F–V bond angles $\sim 135^\circ$, $J_2/k=-0.9$ K) [10]. The M–F–M bond angles in KVF_3 and $RbVF_3$ are 180° and in $NaVF_3$ approximately 148°. In $KVScF_6$ they are approximately 155°. It is not surprising, therefore, that magnetic coupling in $KVScF_6$ (~ 60 K) is closest in temperature to that of $NaVF_3$.

$S=2$: $KCrScF_6$. The fact that the crystal structure of $KCrScF_6$ is tetragonal is surprising since KCr_2F_6 is orthorhombic at room temperature [18]. KCr_2F_6, however, undergoes a Jahn–Teller phase transition to the tetragonal form between 300 and 400 °C [19].

As is the case with the V^{3+} ion, C_M values associated with Cr^{2+} in various fluoride structures differ significantly. In this case, we compare compounds having the general formula $A_xCr_x^{II}Cr_{1-x}^{III}F_3$ (A=K, Rb or Cs; x=0–1), which include the same three structural types. The values of $C_M(Cr^{2+})$ were approximated from the relationship

$$C_M(\text{observed}) = xC_M(Cr^{2+}) + (1-x)C_M(Cr^{3+})$$

In each case, $C_M(Cr^{3+})$ was taken to be 1.88. In the hexagonal bronze phase, Rb_xCrF_3 ($x=0.18$–0.30), the $C_M(Cr^{2+})$ average was 3.27 [20]. For the TTB type phase, K_xCrF_3 ($x=0.43$–0.59), it was 3.80 [18], and for the modified pyrochlore phases Rb_xCrF_3 ($x=0.45$–0.55), 3.02 [21]; and Cs_xCrF_3 ($x=0.45$–0.55), 2.98 [21]. Although $C_M(Cr^{2+})$ for the TTB type phase of K_xCrF_3 (3.80) was larger than that of $KCrScF_6$ (3.25), the difference is probably due to the distortion of K_xCrF_3 from tetragonal to orthorhombic. The average T_N's of hexagonal Rb_xCrF_3 (27 K); orthorhombic K_xCrF_3 (78 K); and modified pyrochlores Rb_xCrF_3 (20 K) and Cs_xCrF_3 (23 K) confirm that the orthorhombic-distorted TTB structure of K_xCrF_3 is at odds with $KCrScF_6$ (intersection of slopes $\sim$23 K).

$S=5/2$: $KMnScF_6$. Divalent fluorides of manganese are in general well behaved. Antiferromagnetic ordering usually occurs within a narrow temperature range: MnF_2 ($T_N=67$ K) [22], $NaMnF_3$ ($T_N=60$ K) [23], $KMnF_3$ ($T_N=88$ K) [24], and $RbMnF_3$ ($T_N=83$ K) [25]. Magnetic coupling in $KMnScF_6$ (intersection of slopes $\sim$50 K) is consistent with magnetic coupling temperatures in these compounds.

5. Conclusion

Perhaps the most important aspect of this work is that these solid state systems can be designed to form specific linear trimers. Most molecular complexes can accommodate only one specific transition metal ion. It is significant that fluoride analogs of TTB can accommodate most of the +2 and +3 first row transition metal ions. Thus, it was possible to select ions with spins of 1/2, 1, 3/2, 2, and 5/2, combined with an appropriate diamagnetic ion, to form linear trimers in these five cases.

Appendix A. Supplementary materials

Supplementary data associated with this article can be found in the online version at doi:10.1016/j.jssc.2010.05.030.

References

[1] A. Magneli, Ark. Kemi 1 (1949) 213.
[2] E. Banks, S. Nakajima, J.B. Williams, Acta Crystallogr. B35 (1979) 46.
[3] Y.S. Hong, R.F. Williamson, K.N. Baker, T.Y. Du, S.M. Seyedahmadian, W.O.J. Boo, Inorg. Chem. 31 (1992) 1040.
[4] R.F. Williamson, K.N. Baker, W.O.J. Boo, Mol. Cryst. Liq. Cryst. 107 (1984) 211.
[5] A.P. Ginsberg, R.L. Martin, R.C. Sherwood, Inorg. Chem. 7 (1968) 932.
[6] Y. Oka, K. Inone, Chem. Lett. 33 (2004) 402.
[7] F.E. Mabbs, D.J. Machin, in: Magnetism and Transition Metal Complexes, Chapman and Hall, London, 1973 (a) p 196, (b) p 177.
[8] K.J. Kambe, Phys. Soc. Jpn. 5 (1950) 48.
[9] R.L. Carlin, A.J. van Duyneveldt, in: Magnetic Properties of Transition Metal Compounds, Springer-Verlag, New York, 1973 (a) pp 1–7 (b) p 118.
[10] J.W. Stout, W.O.J. Boo, J. Chem. Phys. 71 (1979) 1.
[11] W.O.J. Boo, J.W. Stout, J. Chem. Phys. 71 (1979) 9.
[12] S.M. Eicher, J.E. Greedan, J. Solid State Chem. 52 (1984) 12.
[13] Y.S. Hong, R.F. Williamson, W.O.J. Boo, J. Inorg. Chem. 20 (1981) 403.
[14] Y.S. Hong, R.F. Williamson, W.O.J. Boo, J. Inorg. Chem. 19 (1980) 2229.
[15] Y.S. Hong, R.F. Williamson, W.O.J. Boo, J. Inorg. Chem. 21 (1982) 3898.
[16] C. Cros, R. Feurer, M. Pouchard, Mater. Res. Bull. 11 (1976) 117.
[17] R.F. Williamson, W.O.J. Boo, Inorg. Chem. 16 (1977) 646.
[18] Y.S. Hong, K.N. Baker, A.V. Shah, R.F. Williamson, W.O.J. Boo, Inorg. Chem. 29 (1990) 3037.
[19] Y.K. Yeh, Y.S. Hong, W.O.J. Boo, D.L. Mattern, J. Solid State Chem. 178 (2005) 2191.
[20] Y.S. Hong, K.N. Baker, R.F. Williamson, W.O.J. Boo, Inorg. Chem. 23 (1984) 2788.
[21] K.N. Baker, Ph.D. thesis (unpublished), University of Mississippi, 1986.
[22] W. O. J. Boo, J. W. Stout, J. Chem. Phys 65 (1976) 3929.
[23] S. J. Pickart, H. A. Alperin, R. Nathans, BNL-7278.
[24] A.J. Heeger, O. Beckman, A.M. Portis, Phys. Rev. 123 (1961) 1652.
[25] D.T. Teaney, V.L. Moruzzi, B.E. Argyle, J. Appl. Phys. 37 (1966) 1122.